CEAS Aeronaut J (2016) 7:677–694
DOI 10.1007/s13272-016-0213-4

ORIGINAL PAPER

Multidisciplinary design and aerodynamic assessment of an agile and highly swept aircraft configuration

C. M. Liersch[1] · K. C. Huber[2] · A. Schütte[1] · D. Zimper[3] · M. Siggel[4]

Received: 17 March 2016 / Accepted: 9 September 2016 / Published online: 1 October 2016

Abstract The characteristics of highly swept aircraft configurations have been studied in a series of consecutive research projects in DLR for more than 15 years. Currently, the investigations focus on the generic SACCON UCAV configuration, which was specified in a common effort together with the NATO STO/AVT-161 task group. This paper is the first one in a series of articles presenting the SACCON-related research work within DLR. First, the article describes the conceptual design studies being performed for this aircraft configuration. At this point the question is raised, whether the simple aerodynamic methods used within conceptual design can be applied to such type of aircraft configurations with sufficient accuracy. Thus, the second part of this article provides a comparison of the aerodynamic characteristics of the SACCON configuration predicted by low- and high-fidelity aerodynamic methods, as well as some results from wind tunnel experiments.

Keywords Conceptual aircraft design · Multi-fidelity · Highly swept aircraft configurations · SACCON · UCAV aerodynamics

This paper is based on a presentation at the German Aerospace Congress, September 22–24, 2015, Rostock, Germany.

✉ C. M. Liersch
carsten.liersch@dlr.de

[1] German Aerospace Center (DLR), Institute of Aerodynamics and Flow Technology, Brunswick, Germany

[2] German-Dutch Wind Tunnels (DNW), Göttingen, Germany

[3] German Aerospace Center (DLR), Program Coordination Defence and Security Research, Cologne, Germany

[4] German Aerospace Center (DLR), Simulation and Software Technology, Cologne, Germany

Abbreviations

C_A	Axial force coefficient [–]
C_D	Drag force coefficient [–]
C_L	Lift force coefficient [–]
C_N	Normal force coefficient [–]
C_S	Body-fixed side force coefficient [–]
C_Y	Side force coefficient [–]
C_l	Rolling moment coefficient [–]
C_m	Pitching moment coefficient [–]
C_{mx}	Body-fixed X-moment coefficient [–]
C_{my}	Body-fixed Y-moment coefficient [–]
C_{mz}	Body-fixed Z-moment coefficient [–]
C_n	Yawing moment coefficient [–]
I_{xx}	Mass moment of inertia (X-axis) [kg m^2]
I_{yy}	Mass moment of inertia (Y-axis) [kg m^2]
I_{zz}	Mass moment of inertia (Z-axis) [kg m^2]
V	Freestream velocity [m/s]
p, q, r	Rotation rates (X, Y, Z-axis) [°/s]

Conventions

X, Y, Z	Coordinate system

Symbols

α	Angle of attack [°]
β	Angle of sideslip [°]

1 Introduction

Design and performance assessment of military aircraft configurations is an important topic for the German Aerospace Center (DLR[1]). In a series of consecutive projects, spanning over a period of more than 15 years, the

[1] Deutsches Zentrum für Luft- und Raumfahrt e.V.

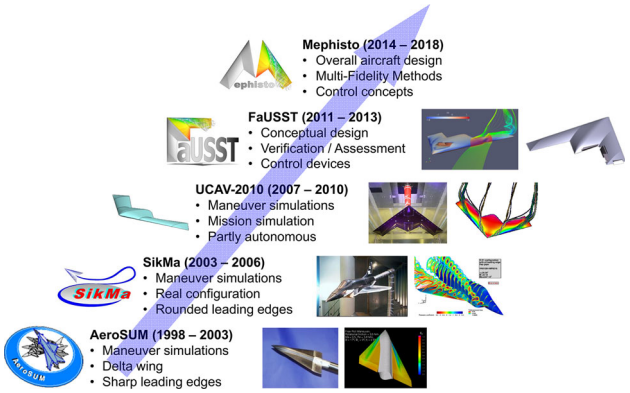

Fig. 1 History of projects dealing with design and assessment of military aircraft configurations

characteristics of highly swept aircraft configurations have been investigated thoroughly (see Fig. 1).

Starting from a generic delta wing configuration featuring sharp leading edges, aerodynamic investigations including maneuver simulations were carried out within the project *AeroSUM*. For the subsequent project *SikMa*, the step towards a realistic and fully equipped fighter aircraft with rounded leading edges was made. At this point it turned out that further investigations required a broader, more multidisciplinary approach, including aircraft design capabilities. Hence, in the successor project *UCAV-2010*, a variety of different disciplines were joined for the design and assessment of a new, generic UCAV[2] configuration. Later, the basic design work for this UCAV configuration was extended by the *FaUSST* project emphasizing on stability and control aspects and linking the different disciplines together in conceptual aircraft design investigations. The current project *Mephisto* focuses on the redesign of the UCAV shape from *UCAV-2010* with enhanced aerodynamic performance and concepts for control and propulsion as key aspects.

The motivation for the previously mentioned DLR projects has to be seen in a broad spectrum of other industrial and research programs. First of all, there is a trend towards unmanned UAV configurations with a low radar signature. This leads to blended wing body configurations without vertical tail planes, like nEUROn (Dassault, [1]), X-47B (Northrop–Grummann, [2]), and Taranis (BAE Systems). Research programs to design the Sagitta configuration (Airbus Defence and Space, [3]) or the 1303 program (US Air Force Research Laboratory, [4]) are focusing on similar planform concepts. The difference between the DLR investigations and some of the other programs might be the particular interest in high agility and high AoA[3] capabilities. Aside from such future configurations, there also is a need for enhanced understanding and prediction capabilities of the characteristics of current fighter type aircraft configurations like the Eurofighter Typhoon (Airbus Defence and Space, [5]). These topics are addressed in the projects described above, as well.

Since the days of *AeroSUM*, the understanding and the prediction capabilities of fighter type aircraft configurations have been considerably extended with respect to detailed flow physics, stability and control behavior, signatures, and aeroelastic characteristics. A variety of components, such as integrated air intakes and nozzles, the propulsion system, or the flight controller has been studied. Starting from *UCAV-2010*, a conceptual design process was built and used for overall aircraft design and assessment studies.

A detailed overview of the specific results from the various investigations performed within the DLR project *FaUSST*, as well as a perspective to its follow-on *Mephisto*, is provided in a series of articles, presented and published in the *DGLR*[4] *Deutscher Luft- und Raumfahrtkongress* in September 2015. While the papers by Huber et al. [6], Schütte et al. [7], and Paul et al. [8] focus on aerodynamics, those by Nauroz [9] and Koch et al. [10] are emphasizing on propulsion and air intake aspects. The one by Voß [11] describes design and sizing of a structural model. Signature investigations are presented in the articles by Lindermeir [12] and Kemptner [13]. Finally, the papers by Schwithal et al. [14] and Kuchar et al. [15] are dealing with flight mechanics assessment and controller development.

This article covers two main topics: the first topic (see Sect. 2) focuses on the conceptual UCAV design system, as well as on its application to the before mentioned UCAV configuration. In the second topic (see Sect. 3), a series of aerodynamic studies is presented. The aim of these studies is to assess the usability of typical conceptual design aerodynamic tools for such a UCAV configuration. The coordinate system and the directions of all force and moment coefficients are shown in Fig. 2. The agility of the aircraft does not stand in the focus of this paper, but it is one of the reasons for the shape of the UCAV configuration being used here.

2 Conceptual UCAV design

The first part of this article is dedicated to conceptual UCAV design. This is an essential capability for DLR, as the development of novel concepts and technologies has to incorporate an assessment of these in the context of a complete aircraft. Furthermore, to come to a realistic

[2] Unmanned Combat Air Vehicle.

[3] Angle of Attack.

[4] Deutsche Gesellschaft für Luft- und Raumfahrt – Lilienthal-Oberth e.V.

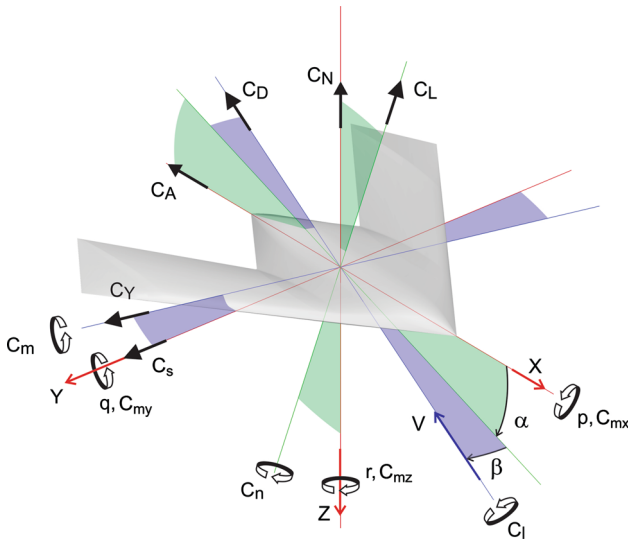

Fig. 2 Coordinate system, see Vicroy et al. [16]

evaluation of the emerging advantages and drawbacks, this complete aircraft has to be optimized such as to exploit the new concept or technology up to a maximum. In Sect. 2.1, the core concept of the applied design system is presented; Sect. 2.2 provides an overview of the design work being performed for the UCAV concept introduced in project *UCAV-2010*.

2.1 Design system

Aircraft design is a highly multidisciplinary task, involving experts from a number of disciplines such as aerodynamics, propulsion, structures, and many others. Even in the early stages of conceptual design it is very useful to have all these experts in the loop. This may help to avoid decisions which may later prove as problematic when looking more into detail. Especially, the discipline of flight mechanics is often introduced at later stages of design since required data regarding aerodynamics, masses, and control surface efficiencies may not be available before. This late-binding of such a crucial discipline has led to a number of substantial problems during the history of aircraft design and should be prevented by providing comprehensive aircraft data as early as possible. Another advantage of early including disciplinary experts and their physics-based tools into the design process becomes apparent when designing unconventional aircraft configurations, such as a highly swept flying wing UCAV. In this case, empirical handbook methods might lead to wrong results if the statistical basis from which they were derived does not cover the designed configuration sufficiently.

The concept to include disciplinary experts, their tools and knowledge even in the very beginning of the design process is one of the core concepts of the aircraft design system being developed by DLR since 2005 [17–19]. The system consists of three parts:

- *Data exchange* A data exchange file format called CPACS[5] is being developed for the DLR aircraft design system [20]. CPACS is an XML based data format which is designed to store aircraft data and geometries in a hierarchical and parametric way. It was introduced mainly to serve as a common language between the disciplinary analysis tools. Two software libraries [21] called TiXI[6] and TiGL[7] are being developed to ease the use of CPACS. TiXI provides a simple interface to create, read, modify, and write XML datasets such as CPACS. The TiGL library generates a 3D CAD[8] model of the aircraft from the parametric data and offers methods to query geometric data from this model. In addition, TiGL provides functions to store the generated geometry to disk using standard CAD exchange file formats. The TiGL viewer application can be used to visualize the underlying CAD model. The complete package of CPACS and libraries is available under open source licenses [22–24].
- *Disciplinary analysis tools* The analysis of an aircraft configuration is performed by disciplinary analysis tools which are provided and maintained by the disciplinary experts. For many disciplines, there is already more than one tool available—each one covering a different level of fidelity or using a different way of modeling. What they all have in common is the need to read and write CPACS datasets as input and output. For new tools, it is certainly a good way to use the CPACS data format directly. For legacy codes, which typically have (and shall keep) their own data formats, the best way is to use a so-called "toolwrapper". A toolwrapper is a small program performing the following steps:
  - Read and process a CPACS file
  - Create an input file for the tool
  - Run the tool
  - Read the output file of the tool
  - Write the results to a CPACS file

  In order to keep the disciplinary experts in the loop and to avoid a decoupling of the used tools from further development, the tools are not gathered at one location to form a monolithic program. Instead, they are placed on disciplinary tool servers which stay under maintenance and supervision of the corresponding experts.

[5] Common Parametric Aircraft Configuration Schema.
[6] TiXI XML Interface.
[7] TiGL Geometry Library.
[8] Computer Aided Design.

Using a software integration framework, these distributed tools can be plugged together to form process chains for aircraft design and analysis.

- *Integration framework* The software integration framework serves as a sort of construction kit. Here, the disciplinary tools, which are located on distributed servers, can be linked together to create customized process chains for particular design or analysis tasks. Trade-study tools, different optimizers and other drivers of the process may be applied to get an impression of the sensitivities of the design parameters, as well as optimal solutions for specific target functions. Up to now, the commercial ModelCenter framework [25] was mainly used for this task, but will be replaced by the DLR integration framework RCE[9] in the future [26]. Just as CPACS, TiXI, and TiGL, RCE is provided under an open source license [27].

This aircraft design system was initially developed for the investigation of commercial transport aircraft. Within the projects *UCAV-2010* and *FaUSST*, it was extended and used for the investigation of a highly swept flying wing UCAV configuration.

2.2 UCAV design

2.2.1 Design specification

With the aim of having a common, generic UCAV concept for research purposes, a new aircraft configuration was introduced in project *UCAV-2010*. While the basic, lambda shaped geometry of this UCAV configuration was oriented towards the typical aim of low observability in combination with high agility, its details were specified in a way such as to have a geometry which could exactly be reproduced in a wind tunnel model as well as in a CFD[10] mesh. Another design aspect was to have a challenging aerodynamic behavior. This was reached by varying the leading edge over wingspan from sharp to round and back to sharp. The design of this, the so-called "SACCON"[11] shape (see Fig. 3), was carried out in a common effort with the NATO STO/AVT[12]-161 task group [28]. The original SACCON geometry has a wingspan of approximately 1.54 m which is well suited to build a wind tunnel model from it. The conceptual design task, presented in this article, was to develop a realistic UCAV concept based upon the original SACCON outer shape. This means that it was only permitted to scale the whole SACCON geometry to a suitable size and to cut out parts for integrating components like control surfaces or engine inlets and nozzles.

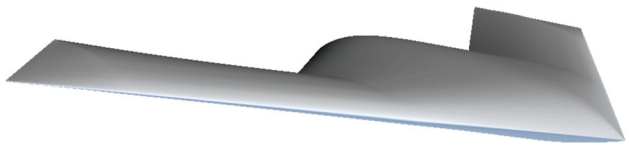

Fig. 3 SACCON outer shape

Table 1 Mission parameters and boundary conditions

Parameter	Value
Outer shape	Scaled SACCON geometry
Propulsion	1 or 2 turbofan engines
Engine integration	buried (due to signature reasons)
Payload storage	Internal (due to signature reasons)
Payload mass	1 × 2000 kg or 2 × 1000 kg
Design range	3000 km (without refueling)
Fuel reserve	≈45 min
Cruise altitude	11 km
Cruise Mach number	0.8 (all altitudes)
Stability margin	2–8 %

In general, each aircraft is designed to fulfill one or more specific design missions. In this context, such a design mission incorporates a payload to be carried and a simplified flight trajectory (consisting at least of altitude and Mach number for a sequence of waypoints). Aside from the mission itself, an aircraft has to meet a number of further boundary conditions like operational requirements and certification rules. For this conceptual design study, only one design mission and a very limited number of additional boundary conditions were specified. The used boundary conditions are composed in Table 1. Figure 4 provides an overview of the design mission profile which was selected for the UCAV.

The payload mass for the UCAV was defined to be 2000 kg in total. Due to signature requirements, an internal storage in one or two payload bays is mandatory. A design range of 3000 km without aerial refueling was considered sufficient—an extra reserve of approx. 45 min is desirable. With this assumption, an operational radius of 1500 km could be reached. Cruise flight to the target area shall be performed at an altitude of 11 km with a Mach number of 0.8. In the target area, the UCAV shall descend to an altitude of 300 m while keeping the Mach number of 0.8. During the last kilometers, it could even descend to 250 m and accelerate to Mach 0.9—but due to the fixed outer shape, this is just an optional requirement. To keep a good maneuverability for this flying wing UCAV without making it laterally unstable, a stability margin of 2–8 % was

[9] Remote Component Environment.

[10] Computational Fluid Dynamics.

[11] Stability And Control CONfiguration.

[12] North Atlantic Treaty Organization, Science and Technology Organization, Applied Vehicle Technology.

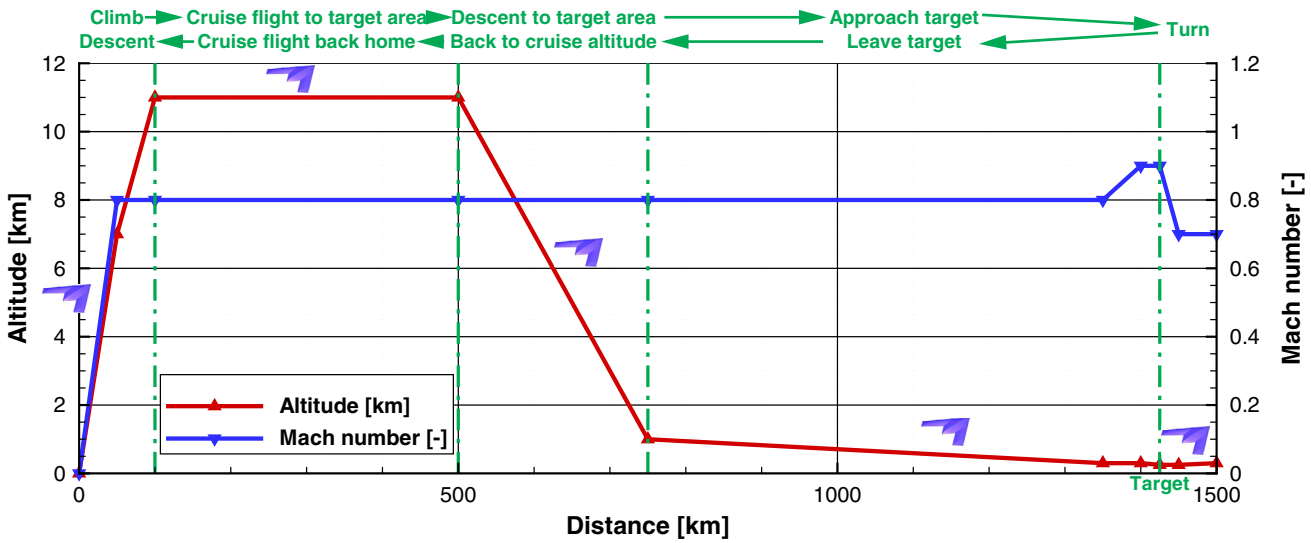

Fig. 4 UCAV design mission

Table 2 Main aircraft parameters

Parameter	Initial	Final
Scaling factor (compared to SACCON)	8.0	10.0
Wingspan	12.3 m	15.375 m
Maximum take-off mass	10.0 t	15.0 t
Thrust-to-weight ratio	0.35	0.4
Static thrust	35.0 kN	60.0 kN

selected. Based on these parameters, an initial estimation of the overall aircraft size and the corresponding take-off mass was made (see Table 2).

These estimated values were used as a starting point for all further investigations and had to be updated during later stages of the design. Based on knowledge from conventional small fighter/trainer aircraft like the Northrop Grumman F5F Tiger II, the thrust-to-weight ratio was set to a relatively small value of 0.35, resulting in a required static thrust of 35 kN. Considering the fixed outer shape which is shown in Fig. 5, a concept with a central payload bay and two engines aside would offer very limited vertical space for the engines, thus permitting only a low bypass ratio. Some preliminary studies showed that such a configuration would need a much larger scaling factor to store enough fuel to reach the specified design range. On the other hand, a single engine is more efficient by default and its location in the middle of the aircraft offers much more vertical space. Hence, this concept was chosen for further investigations. The payload bay was split into two parts which were placed on either side of the engine.

After defining the starting point, the concept was investigated using the DLR conceptual design system. An engine with the required thrust and diameter was designed

Fig. 5 SACCON front view

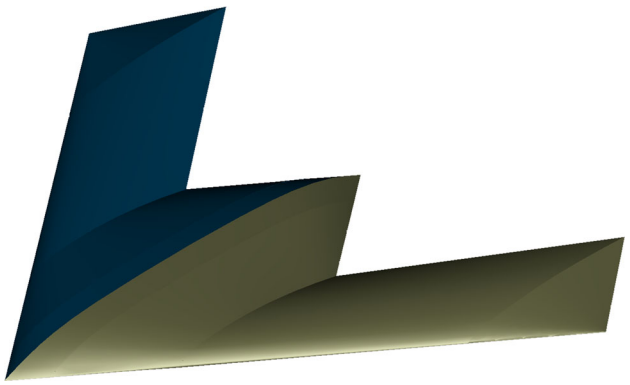

Fig. 6 UCAV CPACS geometry model

especially for this configuration and was included alongside the structural topology and other main components of the UCAV. Using the SACCON CAD geometry together with the already defined parameters, a CPACS model of the UCAV was created. This CPACS model, visualized by the TiGL Viewer in Fig. 6, was used as a central data repository being filled up during the design process.

Furthermore, a Microsoft Excel spreadsheet with a 2D planform view of the geometry and its main components was created to calculate mass breakdown, center of gravity (CG) location, and mass moments of inertia. To be able to investigate changes in center of gravity locations and available fuel volume with respect to parameter changes, it was decided to integrate this spreadsheet directly into the process chain—even though it is limited to configurations

which are quite similar to the current concept. In the future, a more common tool with similar features is expected to be available within the DLR design system.

2.2.2 Design process

Figure 7 illustrates the complete design process, as it was created for the UCAV design task: starting from the CPACS source dataset (upper left corner), the workflow splits up into two main branches, which are computed in parallel, and a third branch (upper right corner). The latter is just responsible for visualizing the current geometry using TiGL functionalities.

The first (left) one of the two branches creates a performance deck for the engine. This performance deck contains all relevant engine parameters (e.g., mass flows, temperatures, emissions) over a variety of flight levels, Mach numbers and thrust settings. The propulsion tool "TWdat" which is used here is a database, fed with a number of engines in advance. The engine design itself is performed separately in the gas turbine simulation environment [29].

The second branch (middle) creates a set of aerodynamic performance maps:

- *Clean performance map* The first performance map contains force and moment coefficients over a variety of Mach numbers, Reynolds numbers, angles of sideslip, and angles of attack, computed for the "clean" configuration without control surface deflections.
- *Control surface delta performance maps* On top of this four-dimensional clean configuration dataset, a five-dimensional delta-coefficient performance map is created for each single control surface (introducing the control surface deflection as fifth dimension). By superposition of different control surface delta coefficients with the absolute coefficients of the clean configuration dataset, it is possible to combine the deflections of multiple control surfaces.
- *Damping derivative performance map* Additionally, an aerodynamic performance map containing the 18 damping derivatives (six force- and moment coefficients, three rotational axis') for each point of the clean configuration dataset is computed.

Depending on the number of each of the dimensions' entries and on the number of control surfaces, this aerodynamic dataset may grow quite large. In fact, for the example presented here, it contains a number of 57,600 entries in total. Even with modern computer systems it is not possible to handle such a number of RANS[13]-CFD computations in an acceptable timeframe—but using simple, potential flow theory based aerodynamics methods, such a performance deck can be created within a few hours or even within minutes. In this process chain, Analytical Methods' commercial "VSAERO" tool [30] is used in combination with DLR's simple "HandbookAero" method which accounts for skin friction drag and wave drag. Other tools, like DLR's open source "LIFTING_LINE" method [31, 32], could be used here as a replacement for VSAERO as well. The question about the limitations of potential flow methods and whether they can be used to model such a configuration and the associated flow physics will be discussed in Sect. 3.

The results of the propulsion and aerodynamics branches are both joined together into the CPACS dataset and handed over to the "TotalMassCoG" script. Furthermore, the engine's mass and position are directly inserted into the Excel spreadsheet described above. The TotalMassCoG script imports mass data, center of gravity location and mass moments of inertia from this Excel spreadsheet and writes them into the CPACS dataset, as well. So, at this point of the process chain, the dataset contains updated performance maps and total mass data.

The following block is an iterative loop which calculates required fuel, landing gear mass, and structural mass:

The left branch contains the tool "flightSimulation" which simulates a flight of the aircraft as specified in the design mission [33]. As a result, the flight trajectory and the required fuel are written back to the CPACS file.

In the second branch, a script selects critical flight loadcases which are then calculated by the connected aerodynamic tools. Again, VSAERO and HandbookAero are used here, but in this case, the output of the aerodynamic tools is a number of spanwise distributions of the aerodynamic coefficients which can be used for structural sizing.

In parallel to the first two branches, the right branch uses the tool "LGDesign" to analyze and size the landing gear [34]. As a result, it provides landing gear mass, as well as critical ground loadcases.

Ground loadcases and landing gear mass are then combined with the spanwise aerodynamic coefficient distributions from the flight loadcases and fed as an input into the structural sizing tool "ModGen". ModGen creates a structural model of the UCAV and sizes the thicknesses of the elements [35].

The computed data for the UCAV's structural mass are combined with the fuel mass from the first branch to a resulting UCAV model. Finally, the so-called "Converger" module checks whether the resulting masses differ significantly from the ones used at start of the iteration loop, and if necessary, it updates the Excel spreadsheet and starts the next iteration.

When the iteration finally has converged, a subsequent analysis process is started: In this case, the flight

[13] Reynolds-averaged Navier–Stokes equations.

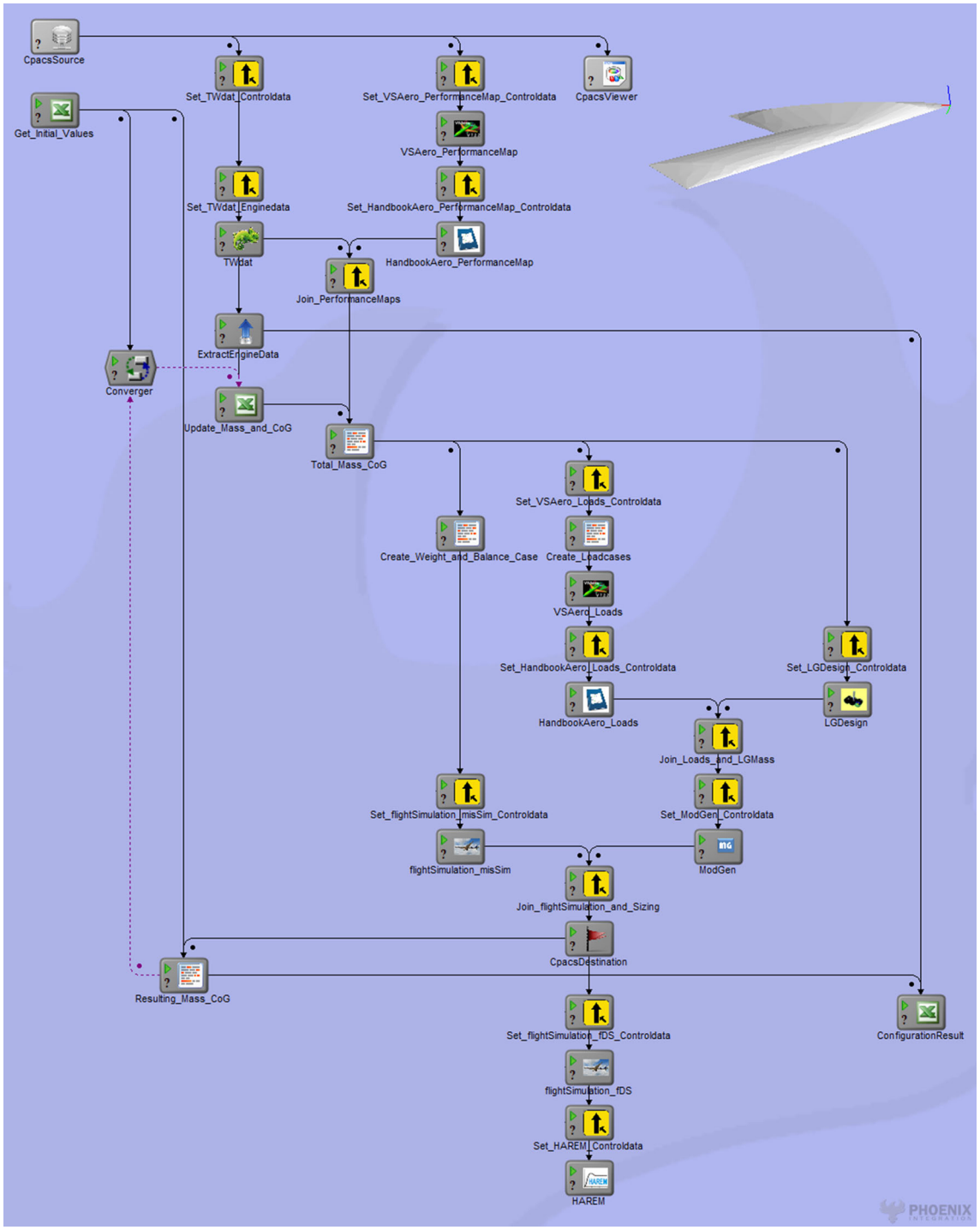

Fig. 7 Conceptual design process (ModelCenter)

Simulation tool is used again, but this time it creates a dynamic aircraft model which is handed over to the "HAREM" tool. HAREM is an analysis tool for investigating and evaluating the handling qualities of an aircraft [14, 36, 37].

The whole process chain was created using DLR's conceptual design system and runs completely automatically. In this case, it uses the ModelCenter integration framework for tool coupling and data exchange. Aside from small scripts and other supporting components, it contains seven different disciplinary tools (three of them are even used twice in different working modes), residing on six servers, provided by five DLR Institutes, located at four different sites distributed over Germany.

Table 3 Engine parameters

Parameter	Condition	Unit	Initial	Final
Static thrust	Take-off	kN	35.0	60.0
Bypass ratio	Cruise flight	–	1.56	3.78
Overall pressure ratio	Take-off	–	28.8	27.65
Mass flow	Take-off	kg/s	60.8	149.05
Turbine entry temperature	Take-off	K	1819	1836
Specific fuel consumption	Cruise flight	g/(kNs)	22.82	20.03
Fan diameter	All	m	0.65	1.12
Length	All	m	2.0	2.3
Weight	All	kg	700.0	1100.0

2.2.3 Design results

As a result from running the process chain, it became obvious that the required fuel volume was nearly two times the available fuel tank volume. Furthermore, it turned out that the payload bays would roughly need twice of the volume available and that the maximum take-off mass would significantly exceed the estimated amount of 10 metric tons. As a consequence, the initially estimated parameters had to be revised: A second global scaling step—this time with a factor of 1.25 (meaning a factor of 10 compared to the initial SACCON geometry in total) and a new maximum take-off mass of 15 metric tons seemed promising here (see Table 2). After this resizing process, the engine had to be redimensioned as well. Taking this as an opportunity, the trust-to-weight ratio was also slightly increased to 0.4. The revised engine uses the extra space for a higher bypass ratio and provides increased thrust as required while showing much lower specific fuel consumption. Main parameters of both engine designs are provided in Table 3 below.

With this new aircraft size, the Excel spreadsheet was used to arrange the inner components in more detail so as to get the landing gear in the right place, to provide enough volume for fuel tanks, and to find good locations for the other main components. The major task of this design step was to limit the longitudinal movement of the center of gravity to stay within the desired stability margins. Especially, the highly swept fuel tanks with their long lever arm and a fuel mass which is nearly half of the take-off mass caused problems. By introducing a second pair of fuel tanks far in front of the center of gravity and by cutting the rear outer parts of the wing tanks, this stability problem could finally be solved. Positioning the payload bays close to the center of gravity further reduced the movement of the aircraft's center of gravity. A snapshot from the Excel spreadsheet showing the UCAV's main components and center of gravity locations after their rearrangement, but before starting the process chain is provided in Fig. 8 (including "DETAIL-A"). During the process, the initially estimated masses were continuously changing until the iteration loop converged. After achieving convergence, the final center of gravity locations (take-off mass for design mission without reserve fuel) are shown in "DETAIL-B" of Fig. 8.

One drawback of this Excel spreadsheet is that it does only contain a 2D model of the inner geometry, whereas the thickness of the UCAV varies continuously over the chord. As a consequence, it is not possible to determine from this model, whether a component really fits into the outer shape. As a solution to this problem, the spreadsheet was extended by a construction table for the CATIA CAD software (Dassault, [38]). Combined with an existing CAD model of the UCAV's outer shape, the CATIA software uses the construction table to generate the inner components as specified in the Excel spreadsheet. Each time the spreadsheet changes during the progress of the process chain, the corresponding CATIA model is updated automatically as well. The CATIA 3D model of the UCAV configuration with its main components is shown in Fig. 9.

A mass breakdown of the UCAV is provided in Table 4. It contains the masses of the main components, their center of gravity locations in *X*-direction and the mass moments of inertia for the main axis'. The deviation moments are currently neglected, as well as the center of gravity locations in *Z*-direction (set to zero). The table is taken from the Excel spreadsheet after running the process chain and shows the case of take-off mass with full payload bays and fuel for the design mission (but excluding reserve fuel). For this mission, the available fuel tank volume is used only by 84.4 %. Taking an average fuel burn per time over the complete mission, the remaining 15.6 % fuel volume ($\approx$950 kg) would equal to an additional flight time of approximately 37 min. If using the extra fuel to extend the high altitude cruise flight section (which is the most efficient flight phase), the additional flight time would increase to approximately 44 min. So, the desired fuel reserve of about 45 min was finally met quite well. In the latter case,

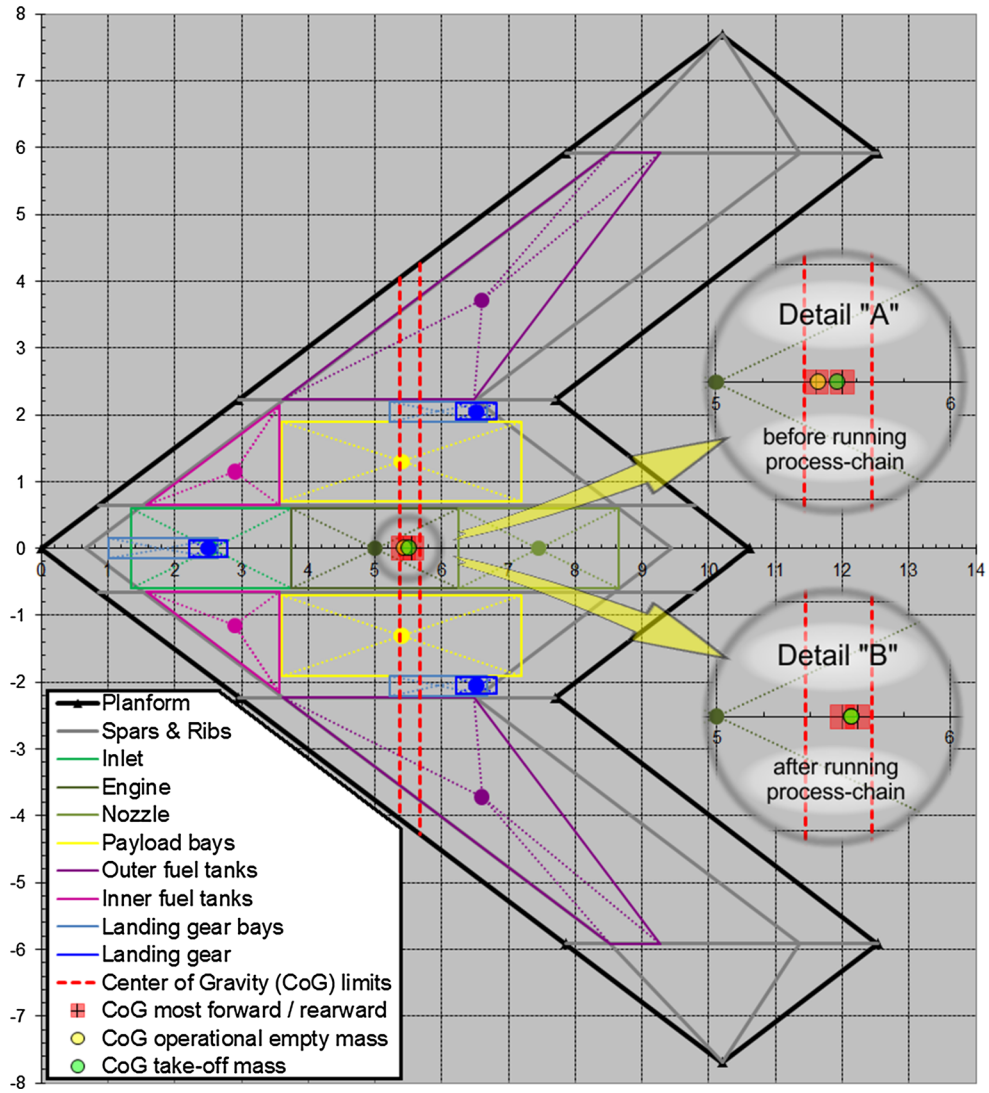

Fig. 8 Main components of the UCAV configuration

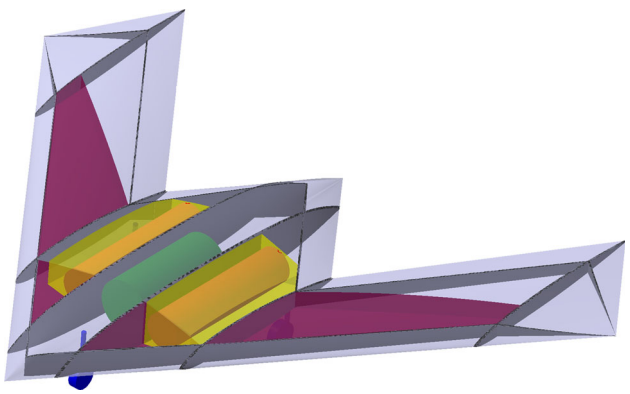

Fig. 9 UCAV 3D view with inner components (CATIA)

the take-off mass would increase to 15.15 metric tons, meeting the initially assumed 15.0 metric tons quite well, too.

The result from simulating the design mission with the final UCAV configuration is depicted in Fig. 10. It shows altitude, angle of attack, Mach number and fuel flow over the mission duration and can be used to get a more detailed insight to the flight trajectory.

3 Aerodynamic analyses

The conceptual design workflow described in the previous section needs an extensive amount of aerodynamic data for performance and load investigations. This database is currently created using simple and fast aerodynamic methods like VSAERO (used for the design study described in Sect. 2.2), or LIFTING_LINE. VSAERO is a 3D singularity method based on the inviscid and incompressible potential flow theory, calculated on surface meshes. For investigating

Table 4 Mass, CG location, and mass moments of inertia around CG

Component	Mass [kg]	CG coordinates			Mass moments of inertia (CG)		
		X [m]	Y [m]	Z [m]	I_{xx} [kgm^2]	I_{yy} [kgm^2]	I_{zz} [kgm^2]
Structures	2677	6.33	0.00	0.00	30,486	3436	33,922
Landing gear	496	5.63	0.00	0.00	1514	1441	2955
Propulsion	1541	5.40	0.00	0.00	0	677	677
Systems	1790	4.65	0.00	0.00	0	7627	7627
Other	559	5.42	0.00	0.00	760	23	783
Empty mass	**7062**	**5.58**	**0.00**	**0.00**	**32,760**	**13,204**	**45,964**
Payload	2000	5.40	0.00	0.00	3380	62	3442
Forward CG	**9092**	**5.54**	**0.00**	**0.00**	**36,140**	**13,267**	**49,407**
Fuel	5140	5.64	0.00	0.00	58,498	19,350	77,849
Rearward CG	**12,202**	**5.61**	**0.00**	**0.00**	**91,258**	**32,555**	**123,813**
Take-off mass	**14,202**	**5.58**	**0.00**	**0.00**	**94,638**	**32,617**	**127,255**

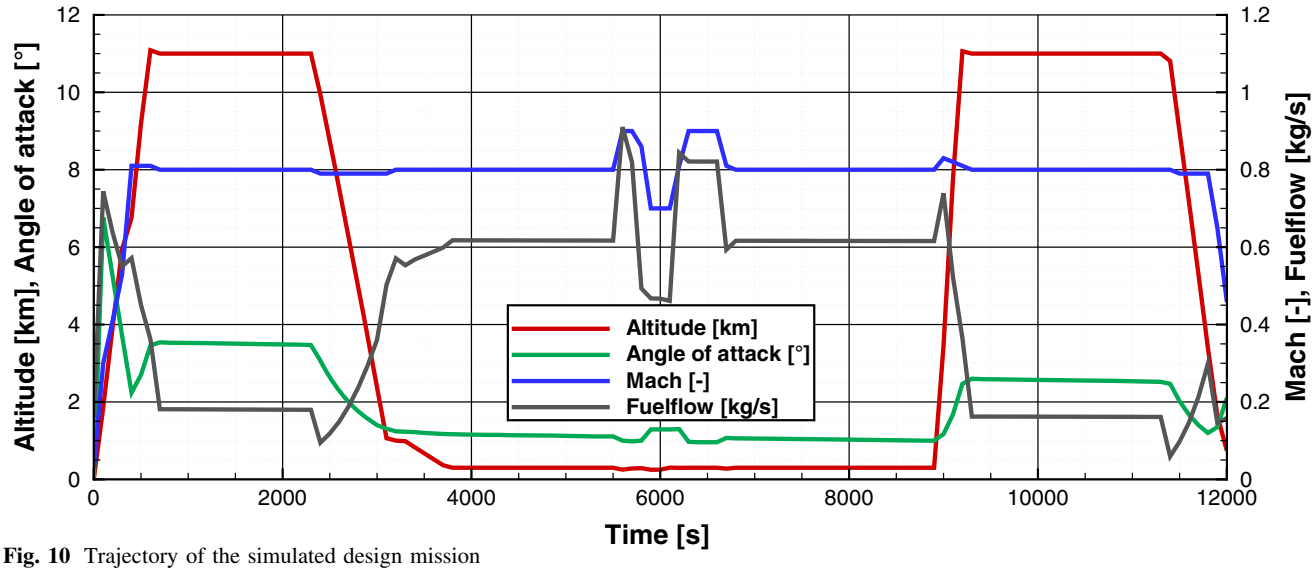

Fig. 10 Trajectory of the simulated design mission

compressible flows, several compressibility corrections are included; viscous drag can optionally be considered through an iteratively coupled boundary layer module. LIFTING_LINE is running faster than VSAERO, but is based on the even more simplified skeleton theory (also called camberline theory). In skeleton theory, the 3D surface is reduced to a set of flat panels; hence it neglects all effects coming from thickness. Further simplifications include a limitation to small angles of attack and sideslip. For compressible flows, LIFTING_LINE offers a compressibility correction, as well. Over the years, VSAERO and LIFTING_LINE are well proven for investigating conventional transport aircraft configurations.

The question now is: how far can these simple methods are used for a highly swept flying wing aircraft? It is doubtless that the simple theory behind these tools is not able to model the complex vortex systems occurring for such aircraft, especially at higher angles of attack. On the other hand, this simple theory is known to behave conservatively in most cases. So the calculated loads are expected to be typically larger than what really will appear at the aircraft. In fact, this would conservative in terms of structural sizing, but this also would mean that control surface efficiencies might actually be much lower than predicted. In this chapter, results from VSAERO and LIFTING_LINE will be compared to the measurements of the DLR-F19 wind tunnel model (which was built from the SACCON geometry) [39–41] and to RANS results created with the "DLR-TAU" code [42–45]. The flow conditions for the comparison at subsonic speed are defined by the wind tunnel experiment: Mach number is 0.15, Reynolds number is 1.6×10^6, based on the DLR-F19 reference chord length. For the comparison

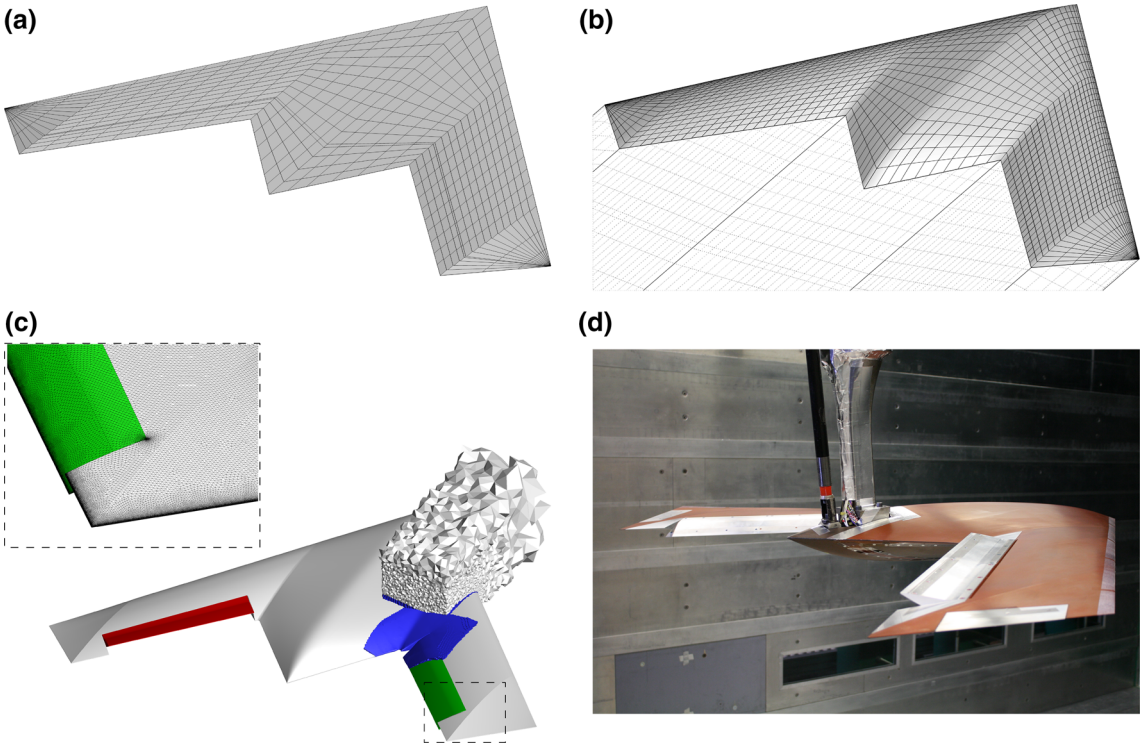

Fig. 11 Aircraft models for computation and wind tunnel measurements. **a** LIFTING_LINE mesh. **b** VSAERO mesh. **c** Tau mesh. **d** DLR-F19 wind tunnel model

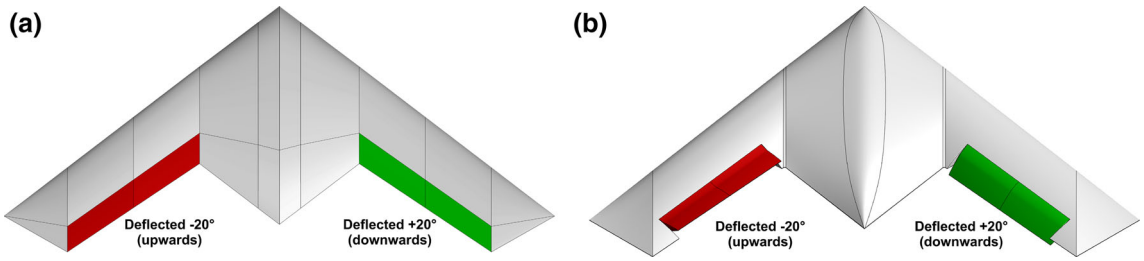

Fig. 12 Differences in control surface geometry. **a** LIFTING_LINE and VSAERO. **b** Tau and wind tunnel model

at transonic speeds, real flight conditions of the initial full-scale configuration have been considered (see Table 2, initial design with a scaling factor of 8): Mach numbers are 0.55, 0.8, 0.85, Reynolds number is 23×10^6.

TAU is a CFD tool developed by the DLR Institute of Aerodynamics and Flow Technology. It solves the compressible, three-dimensional, time-accurate RANS equations using a finite volume formulation. The code is based on a hybrid unstructured-grid approach, which makes use of the advantages that prismatic grids offer in the resolution of viscous shear layers near walls, and the flexibility in grid generation offered by unstructured grids. The TAU computations for this study were performed using the SA[14] turbulence model at subsonic speed, as well as at transonic speeds. Details about this model and the complete computational setup can be found in Schütte et al. [46] and Zimper et al. [47]. As the LIFTING_LINE computations are performed inviscid, the HandbookAero tool is applied afterwards to incorporate the turbulent viscous drag using the method of the equivalent flat plate. For a better comparison, VSAERO is utilized twice here: once using its own boundary layer module and once without that module, applying HandbookAero as it is done for LIFTING_LINE. The computational meshes of the three aerodynamic methods are depicted in Fig. 11, together with a picture of the DLR-F19 wind tunnel model.

Control surface deflections in LIFTING_LINE and VSAERO are modeled just by rotating the normal vectors of the corresponding wing panels—but without changing the geometry itself. In LIFTING_LINE, the hinge line for control surface deflection is always projected into the global *Y*–*Z*-Plane before use. This simplification of course leads to

[14] Spalart–Allmaras.

slightly different results, which will be discussed below. In the 3D TAU mesh (as well as in the wind tunnel model), the control surfaces are deflected geometrically, but without a gap. Figure 12 shows the control surface geometry used for LIFTING_LINE and VSAERO (left) and for TAU and the wind tunnel model (right). On each side, there are two control surfaces: one inboard and one outboard. Regarding the side edges, the control surface definition used for LIFTING_-LINE and VSAERO is not able to model the geometry from the wind tunnel exactly. The simplification, which is currently used even leads to slightly bigger control surfaces and will certainly produce a small overprediction of control surface effects.

3.1 Subsonic Speed

Figure 13 shows a comparison of the aerodynamic coefficients of the clean configuration for angles of attack from 0° up to 15°. As can be seen, the LIFTING_LINE and VSAERO results generally do agree quite well. As expected, VSAERO VISCOUS exhibits a slightly lower lift curve slope due to the viscous effects and a far too low drag coefficient due to the fact that the computation was performed with free transition, resulting in a partial laminar boundary layer. For the pitching moment curves, they show a slight deviation, especially for higher angles of attack. However, since the moment reference point is located very close to the neutral point, the deviation only means a small discrepancy in the position of the neutral point and must not be overestimated. Compared to TAU and the experimental data, the lift curve shows a marginally higher slope (which is typical for potential flow theory) and a minimal shift in the zero-lift angle. The drag curve of the TAU results differs significantly from the experimental results. The reason for this deviation is the influence coming from the sting of the wind tunnel model. This was shown by a TAU simulation including the sting, performed by Schütte et al. [46]. For angles of attack up to 10°, the drag curves of LIFTING_LINE and VSAERO are in good agreement with the TAU results; for higher angles of attack, the drag is under-predicted by them, as the complex flow characteristics cannot be modeled sufficiently. In terms of pitching moment, there is again a strong deviation between TAU results and experimental data—especially for higher angles of attack. This effect is due to the experimental set up of the model: The belly sting arrangement of the wind tunnel contributes to the coefficient; the mounting is, however, not modeled in the computation. If modeled, improvements in coefficient prediction can be shown, see Schütte et al. [46]. In this case, a TAU computation with sting reduces the deviation and leads to similar gradients, but there is still an offset left between the two curves. As a reason for this offset, the article [46] suspects that the flow topology coming from the sting is not predicted correctly by TAU. Comparing the pitching moment curves from LIFTING_-LINE and VSAERO to the TAU results, it can be stated that they are in good agreement for low angles of attack. For angles of attack higher than 10°, the discrepancy increases due to vortex effects which are not modeled by the simple methods. Finally, as it should be the case for a symmetrical geometry under symmetrical flow conditions, the side force coefficients are zero—as well as the rolling and yawing moment coefficients.

The effect of deflecting the control surfaces (left side upwards by 20°, right side downwards by 20°) is depicted as difference to the clean configuration (see Fig. 13) in Fig. 14. Generally, it can be stated that the effect on lift, drag, and pitching moment coming from control surface deflection is very small and in good agreement. The rolling moment coefficient offsets of TAU and experiment are nearly constant over the angle of attack and in very good agreement with each other. As expected, the results from VSAERO and LIFTING_LINE are overpredicting this offset significantly. This effect is coming mainly from the 3D flow effects which are reducing the control surface efficiency and which are not modeled by the simple methods. The influence on the yawing moment is generally quite small. The trend of yawing moment development with increasing angle of attack is, however, represented correctly by all numerical methods considered. Here, LIFTING_LINE overpredicts this development significantly, whereas VSAERO under-predicts it. Some small side force is existent in the experiments, which is predicted well by the TAU results. VSAERO increasingly overpredicts the side force with increasing angle of attack, though gives rise to the correct sign. One possibility, which will be further investigated in the future, could be that this effect is coming from mesh resolution and computational accuracy. LIFTING_LINE here gives rise to a strongly overpredicted side force, which is even of opposite sign. The reason for this effect is that the simple geometry model consisting of flat plates with a slight dihedral due to wing twist creates an unrealistic side force, being proportional to the angle of attack.

Looking at isolated control surface deflection cases, the same trends as for the combined deflections described above can be found. However, looking at higher angles of attack, the delta coefficients from TAU and experiment are not identical to the sum of isolated inboard and outboard delta coefficients. This means that the highly swept UCAV control surfaces are having a significant impact on each other due to 3D flow effects. Therefore, the combination of isolated control surface deflections by superposition of their delta coefficients—as commonly used for transport aircraft with a lower wing sweep—is not sufficient for high angles of attack. LIFTING_LINE and VSAERO are not

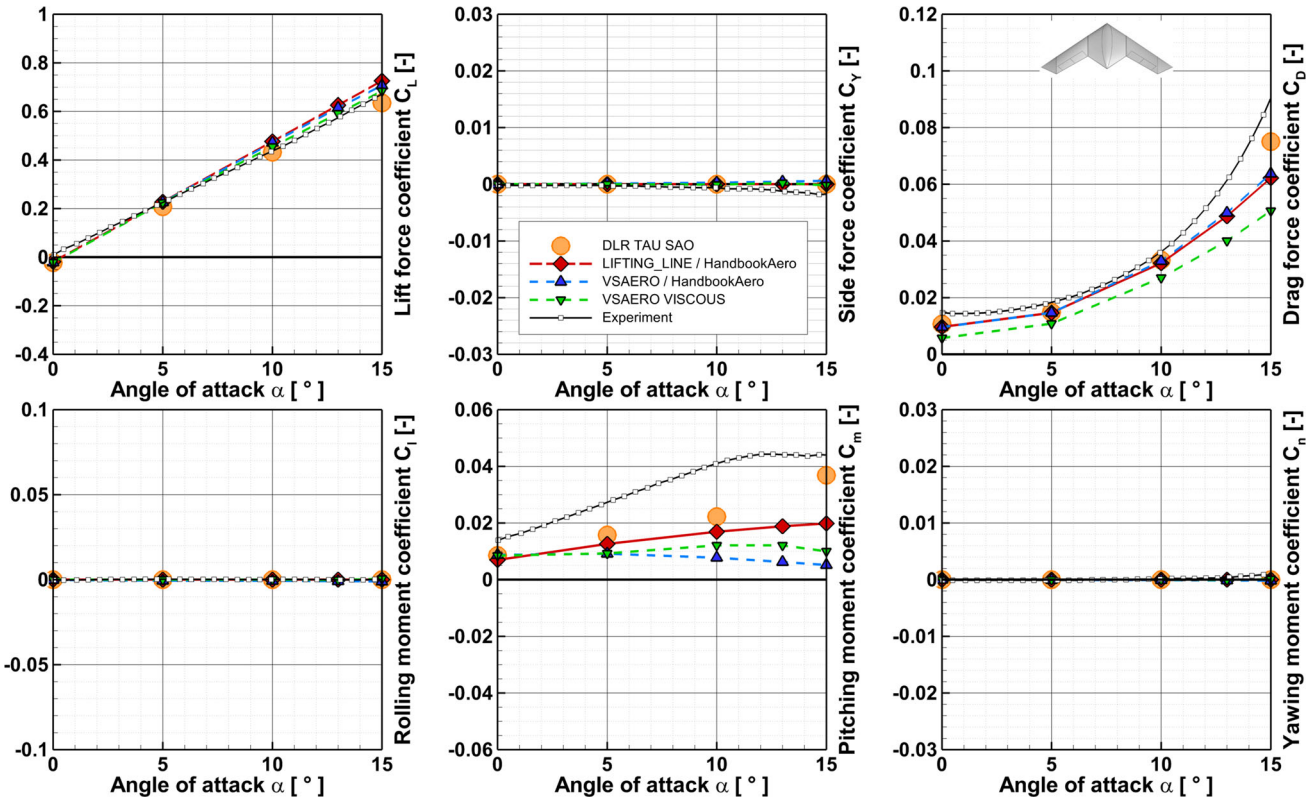

Fig. 13 Total coefficients of clean configuration ($M = 0.15$, $RE = 1.6 \times 10^6$, α variation, $\beta = 0°$)

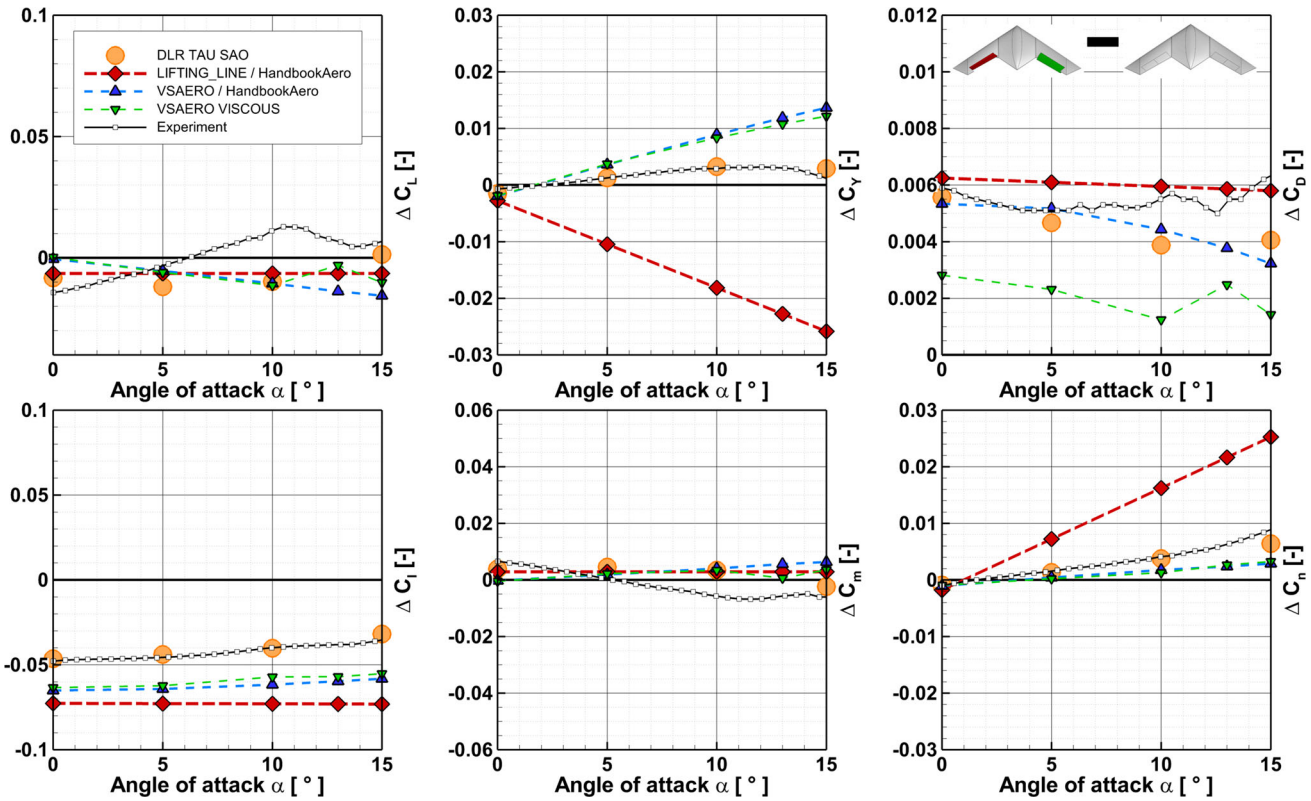

Fig. 14 Delta coefficients due to deflected inboard and outboard control surfaces. ($M = 0.15$, $RE = 1.6 \times 10^6$, α variation, $\beta = 0°$)

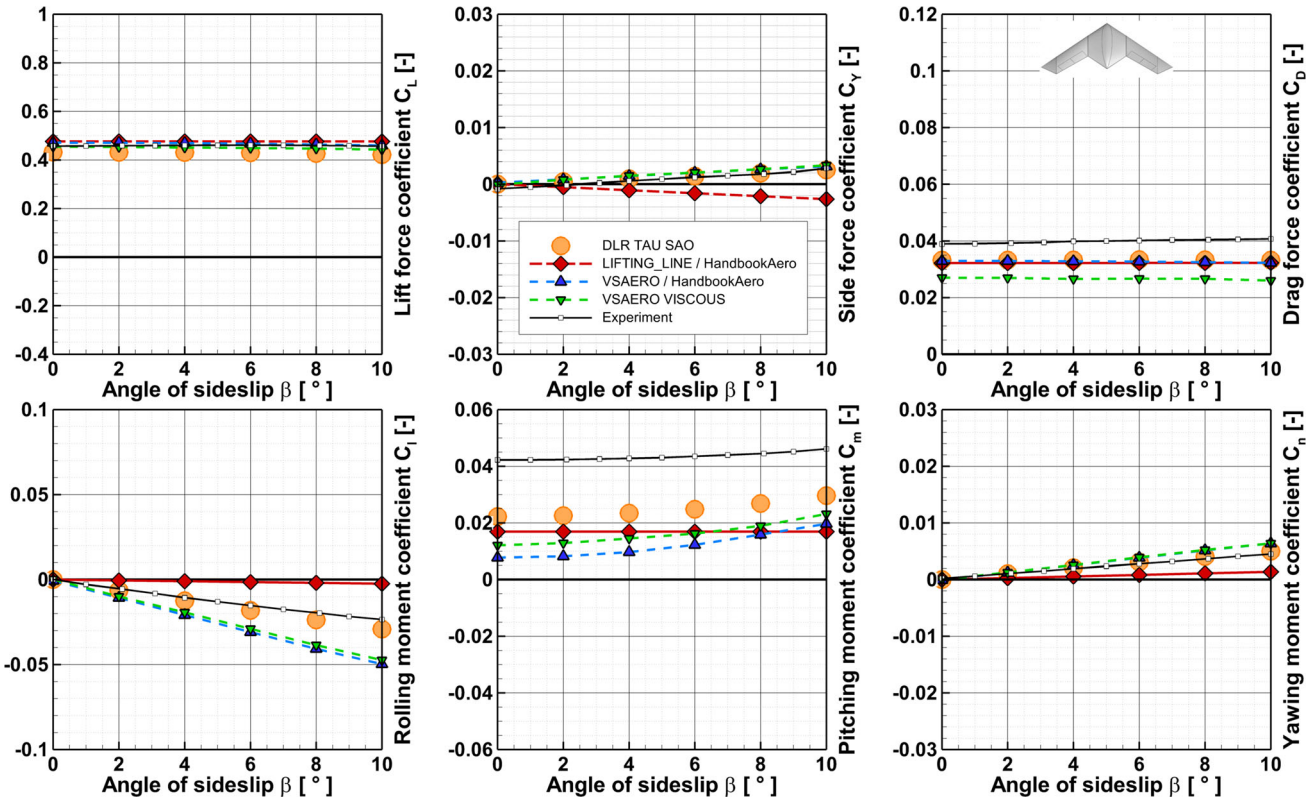

Fig. 15 Total coefficients of clean configuration ($M = 0.15$, $RE = 1.6 \times 10^6$, $\alpha = 10°$, β variation)

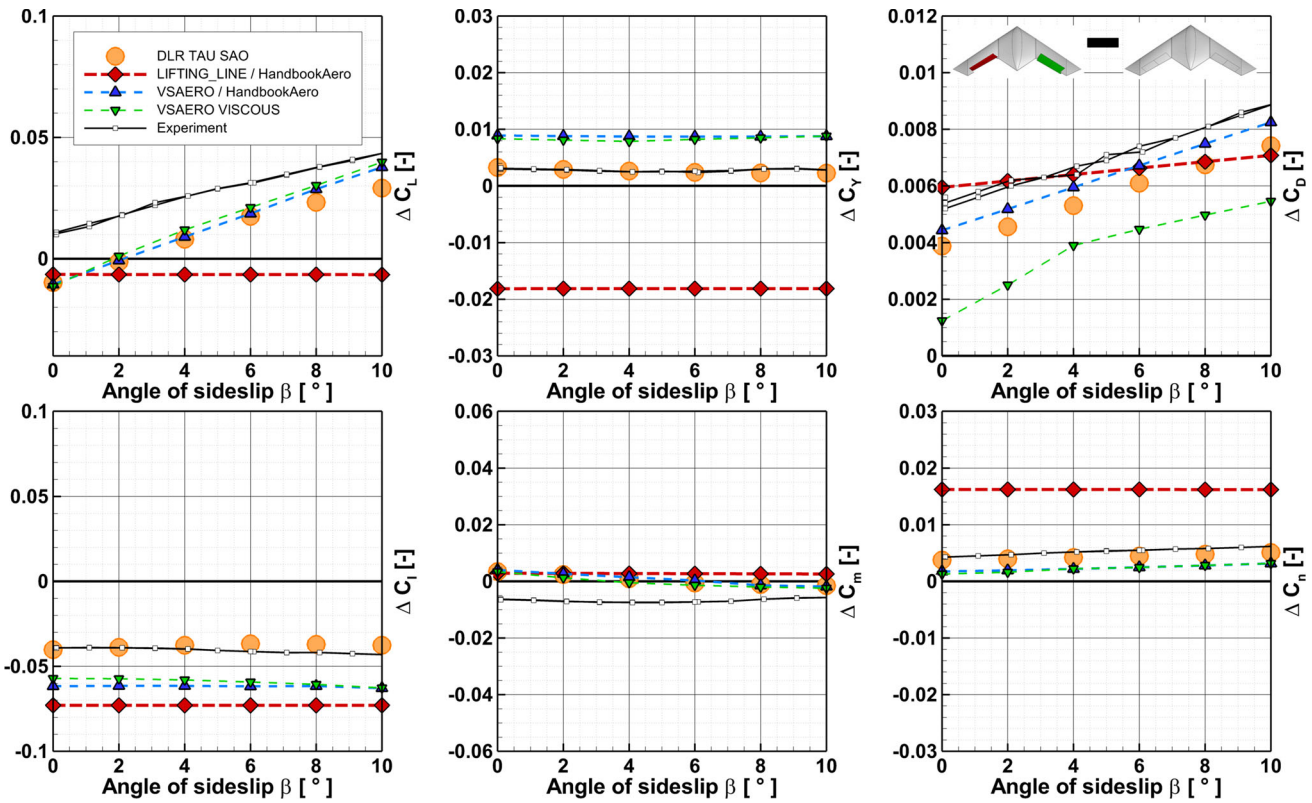

Fig. 16 Delta coefficients due to deflected inboard and outboard control surfaces ($M = 0.15$, $RE = 1.6 \times 10^6$, $\alpha = 10°$, β variation)

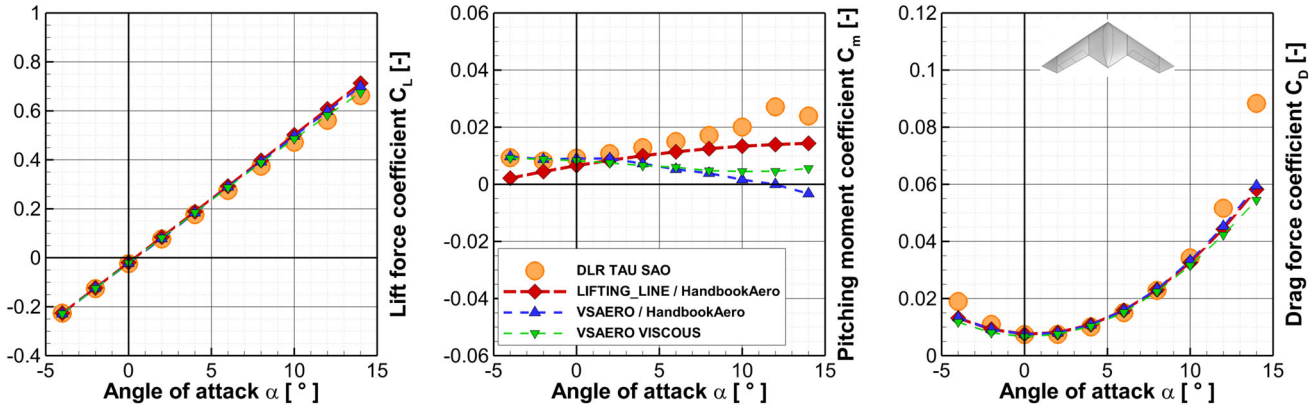

Fig. 17 Total coefficients of clean configuration ($M = 0.55$, $RE = 23 \times 10^6$, α variation, $\beta = 0°$)

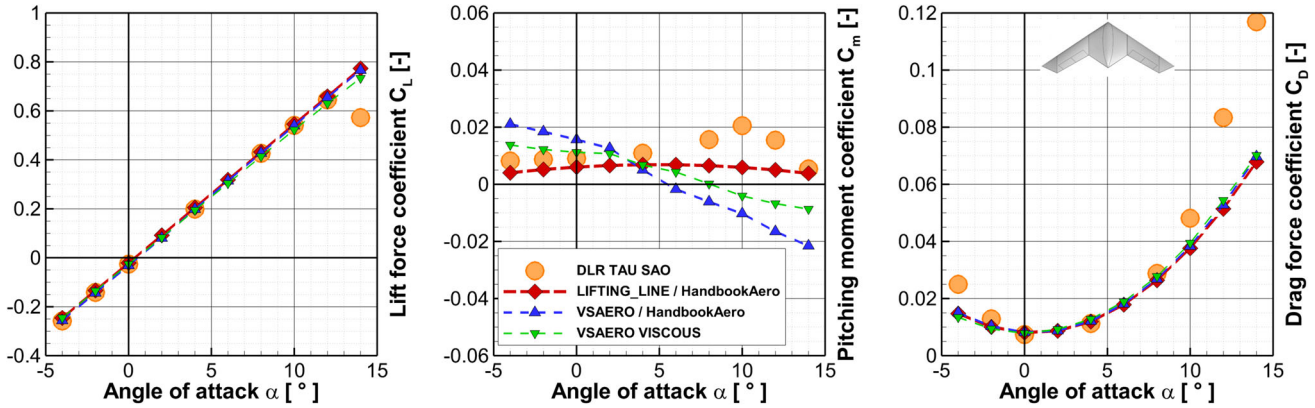

Fig. 18 Total coefficients of clean configuration ($M = 0.80$, $RE = 23 \times 10^6$, α variation, $\beta = 0°$)

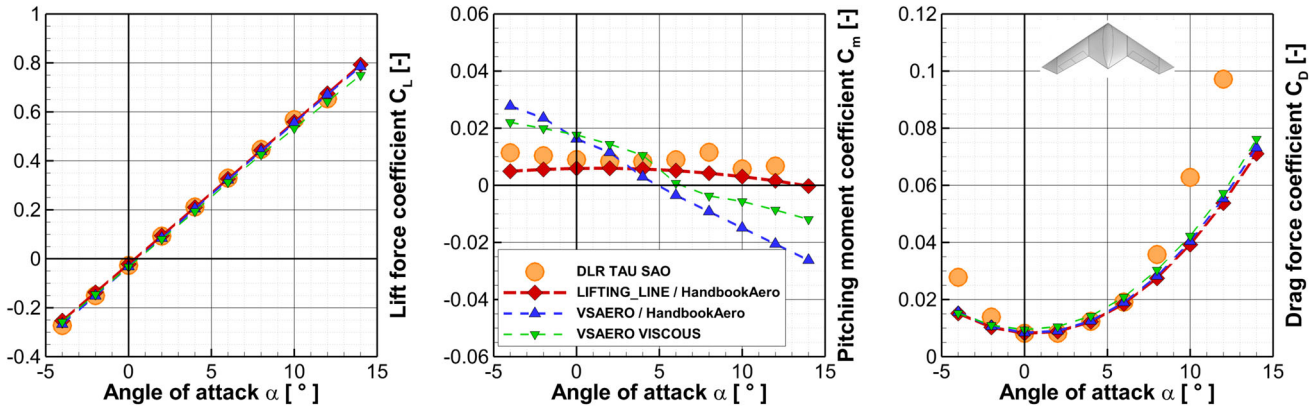

Fig. 19 Total coefficients of clean configuration ($M = 0.85$, $RE = 23 \times 10^6$, α variation, $\beta = 0°$)

predicting this cross-influence. Details about the differences between isolated and combined deflections are discussed by Liersch et al. [48].

In Figs. 15 and 16, the effects due to a sideslip variation are depicted. Figure 15 contains the total coefficients, whereas Fig. 16 display the deltas due to a combined control surface deflection (similar to the one used in Fig. 14). To display the effects clearly, an angle of attack of 10° is chosen. The trends from VSAERO fit well to the results from TAU and from the wind tunnel measurements. The absolute values for the pitching moment are under-predicted; the rolling moment is significantly overpredicted. Taking into account that the absolute values are all quite low here (except for the lift coefficient), the

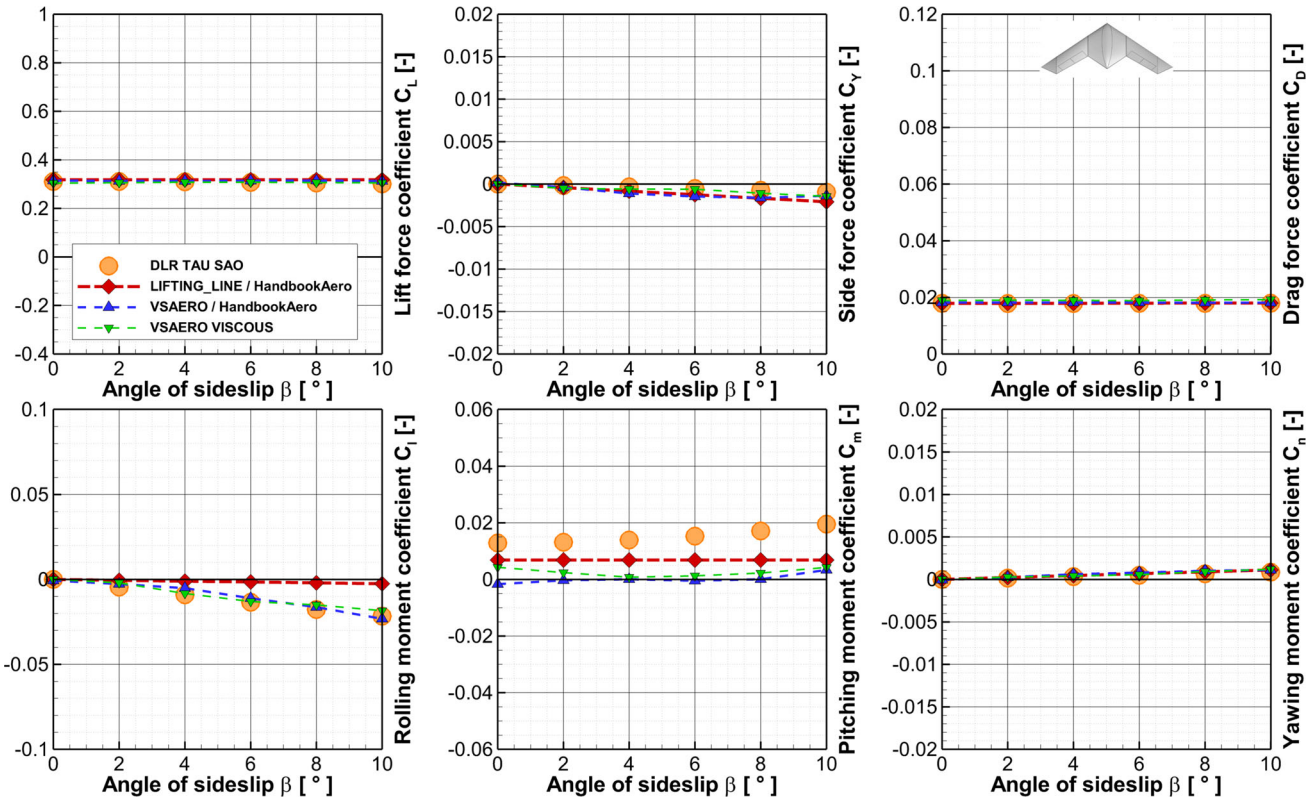

Fig. 20 Total coefficients of clean configuration ($M = 0.80$, $RE = 23 \times 10^6$, $\alpha = 6°$, β variation)

VSAERO results can be considered as sufficient. Regarding LIFTING_LINE, it is obvious that there is nearly no influence from the sideslip angle. This effect is a result from the simplifications described above in combination with the SACCON geometry: Within LIFTING_LINE, the SACCON geometry is nearly a totally flat plate. As the sideslip angle is considered to be small, the flow in X-direction is not reduced due to sideslip. Hence, the rolling moment coming from deflected control surfaces is slightly overestimated and nearly independent from sideslip as well. On the other hand, the component from the incoming flow, which is oriented in Y-direction does not create significant effects because the LIFTING_LINE geometry is nearly flat and the kinematic flow condition for each panel (including control surfaces) is evaluated in the X–Z-plane only. As a consequence, LIFTING_LINE cannot predict the coefficients due to sideslip here.

3.2 Transonic speeds

Figures 17, 18, and 19 show a comparison between LIFTING_LINE, VSAERO and RANS results for a range of angles of attack between −5° and 15° at Mach numbers of 0.55, 0.8, and 0.85.[15] The RANS calculations were conducted with the initial design full-scale configuration without control surface deflections (see Table 2). For all Mach numbers a very good agreement can be seen comparing the results of the lift coefficients up to an angle of attack of 10°. As already indicated for the comparisons at subsonic speed, the nonlinear aerodynamic effects at higher angles of attack cannot be modeled by potential flow theory based methods like LIFTING_LINE and VSAERO. Only the RANS computations are able to simulate the nonlinear vortex flow occurring at an angle of attack greater than 10°. A deviation can be seen between the pitching moment coefficient curves. A different gradient is indicated comparing the slope of the RANS curves with the LIFTING_LINE and VSAERO curves. Taking into consideration the location of the neutral point with respect to the moment reference point, again, the deviation should not be overestimated. As expected, the nonlinear behavior for an angle of attack greater than 10° is not reflected by the LIFTING_LINE and VSAERO curves. The drag coefficient is predicted quite well by LIFTING_LINE and VSAERO. Due to the higher Mach and Reynolds numbers (compared to the low speed study in Sect. 3.1), the laminar flow areas predicted by VSAERO VISCOUS are far smaller, thus resulting in a drag coefficient which is very similar to the one computed using HandbookAero. Just for the combination of high Mach

[15] The Tau RANS result for $M = 0.85$, $\alpha = 14°$ is missing because a converged solution could not be found for that case.

numbers and high angles of attack, the drag coefficients are becoming under-predicted.

Figure 20 shows the aerodynamic coefficients for sideslip angle sweeps at an angle of attack of 6°, a Mach number of 0.8, and a Reynolds number of 23×10^6. RANS results are compared again with LIFTING_LINE and VSAERO results. The agreement between results for the lift, drag, and yawing moment coefficient can be stated as excellent. There is nearly no deviation between the different results. Additionally, it can be seen that an angle of sideslip of up to 10° has no remarkable influence on these three coefficients. With respect to the pitching moment coefficient, there are again significant deviations of LIFTING_LINE and VSAERO from the TAU results, but as already mentioned for the results of the angle of attack investigations, the deviation should not be overestimated due to the location of the neutral point with respect to the moment reference point. Furthermore, VSAERO even predicts the slope of the moment curve quite well. Considering the side force coefficients, a good agreement between the different methods can be stated. The relative difference is quite big, but as the absolute values are very small, this is not considered as a problem here.

4 Conclusion

During a sequence of consecutive projects, the DLR conceptual design system was extended to permit design and analysis of highly swept flying wing UCAV configurations. A UCAV design task based on the generic SACCON geometry, developed together with the NATO STO/AVT-161 task group, was specified and a conceptual design workflow for this task was created. Together with partners from several disciplines, the UCAV design work was performed in a distributed process. A global scaling factor of 10 and an elaborated inner layout were the keys for fulfilling the design requirements. The question, whether simple and fast aerodynamic methods can provide suitable aerodynamic coefficients for such a configuration was investigated by comparison to RANS aerodynamics and wind tunnel measurements under low and high speed conditions. As a result, it can be stated that the coefficients from simple aerodynamic methods can be sufficient as long as the angles of attack are kept low. The effects of deflected control surfaces are typically covered with a slight overestimation, but are still sufficient for low angles of attack, as well. In case of transonic speeds in combination with high angles of attack, suitable wave drag estimation could help to improve the accuracy of the computed drag coefficients. If an emphasis is placed on sideslip in combination with flat aircraft configurations, then the methods that are not neglecting the thickness have to be used. At higher angles of attack, especially the pitching moment from simple methods might develop strong deviations to reality, both in total values and trends. So, a mission analysis for fuel estimation can normally use coefficients from simple methods without problems. For the design of a flight control system or other flight dynamic investigations being performed in the early stages of design, aerodynamic data coming purely from simple methods might not be sufficient. In such cases, a multi-fidelity approach could help to correct thousands of potential flow computations by a few well selected RANS computations or wind tunnel results.

Acknowledgments The design work presented here was performed in close cooperation with DLR-colleagues from all involved disciplines, namely aeroelastics, flight mechanics and systems, infrared-signatures, propulsion, radar signatures, structures, system dynamics and control. The authors would like to thank all colleagues who contributed to this design work. An additional acknowledgement has to be given to the community of the DLR conceptual design system.

References

1. Louis, J., Marchetto, A., Maretsis, M., Mijares, F.: nEUROn: An International Cooperation to Enhance Innovation. ICAS General Lecture, ICAS Congress, St. Petersburg (2014)
2. Jenkins, D.R., Landis, T., Miller, J.: AMERICAN X-VEHICLES—centennial of flight edition: an inventory 2014 X-1 to X-50. Monogr. Aerosp. Hist. 31, SP-2003-4531 (2013)
3. Hövelmann, A., Breitsamter, C.: Aerodynamic Characteristics of the SAGITTA Diamond Wing Demonstrator Configuration. DGLR, Deutscher Luft- und Raumfahrtkongress 2012, Berlin (2013). urn:nbn:de:101:1-2013020112060
4. Woolvin, S.: Conceptual design studies of the 1303 configuration. AIAA 2006-2991, 24th AIAA Applied Aerodynamics Conference, San Francisco, CA, 2006. doi:10.2514/6.2006-2991
5. Rauen, A.: Eurofighter Typhoon. ICAS General Lecture, ICAS Congress, Anchorage (2008)
6. Huber, K., Rein, M., Schütte, A., Löser, T.: Experimental Aerodynamic Assessment and Evaluation of an Agile Highly Swept Aircraft Configuration. DGLR, Deutscher Luft- und Raumfahrtkongress, Rostock (2015)
7. Schütte, A., Huber, K., Zimper, D.: Numerische aerodynamische Analyse und Bewertung einer agilen und hoch gepfeilten Flugzeugkonfiguration. DGLR, Deutscher Luft- und Raumfahrtkongress, Rostock (2015)
8. Paul, M., Rütten, M., Rein, M.: Numerische Untersuchungen von nicht konventionellen Steuerkonzepten für eine agile und hoch gepfeilte Flugzeugkonfiguration. DGLR, Deutscher Luft- und Raumfahrtkongress, Rostock (2015)
9. Nauroz, M.: Antriebskonzept einer agilen und hoch gepfeilten Flugzeugkonfiguration. DGLR, Deutscher Luft- und Raumfahrtkongress, Rostock (2015)
10. Koch, S., Rütten, M., Rein, M.: Experimentelle und numerische Untersuchungen zu integrierten Einläufen für agile und hoch gepfeilte Flugzeugkonfigurationen. DGLR, Deutscher Luft- und Raumfahrtkongress, Rostock (2015)
11. Voß, A.: Design and Sizing of a Parametrized Structural Model for a UCAV Configuration for Loads and Aeroelastic Analysis. DGLR, Deutscher Luft- und Raumfahrtkongress, Rostock (2015)

12. Lindermeir, E., Rütten, M.: Infrarotsignaturbewertung von agilen und hoch gepfeilten Flugzeugkonfigurationen. DGLR, Deutscher Luft- und Raumfahrtkongress, Rostock (2015)
13. Kemptner, E.: Radarsignaturbewertung von agilen und hoch gepfeilten Flugzeugkonfigurationen. DGLR, Deutscher Luft- und Raumfahrtkongress, Rostock (2015)
14. Schwithal, J., Rohlf, D., Looye, G., Liersch, C.M.: An innovative route from wind tunnel experiments to flight dynamics analysis for highly swept flying wing. DGLR, Deutscher Luft- und Raumfahrtkongress, Rostock (2015)
15. Kuchar, R., Steinhauser, R., Looye, G.: Reglerentwurf für eine agile und hoch gepfeilte Flugzeugkonfiguration. DGLR, Deutscher Luft- und Raumfahrtkongress, Rostock (2015)
16. Vicroy, D.D., Huber, K.C., Loeser, T., Rohlf, D.: Low-speed dynamic wind tunnel test analysis of a generic 53° swept UCAV configuration with controls. 32nd AIAA Applied Aerodynamics Conference, No. AIAA-2014-2003, Atlanta, GA, June 2014
17. Liersch, C.M, Hepperle, M.: A unified approach for multidisciplinary preliminary aircraft design. CEAS 2009 European Air and Space Conference, October 2009
18. Liersch, C.M., Hepperle, M.: A distributed toolbox for multidisciplinary preliminary aircraft design. CEAS Aeronaut. J. **2**(1–4), 57–68 (2011)
19. Nagel, B., Zill, T., Moerland, E., Böhnke, D.: Virtual aircraft multidisciplinary analysis and design processes—lessons learned from the collaborative design project VAMP. CEAS 2013 European Air and Space Conference, September 2013
20. Nagel, B., Böhnke, D., Gollnick, V., Schmollgruber, P., Rizzi, A., Rocca, G.L., Alonso, J.J.: Communication in aircraft design: can we establish a common language?. 28th International Congress of the Aeronautical Sciences (ICAS), 2012
21. Bachmann, A., Kunde, M., Litz, M., Schreiber, A.: A dynamic data integration approach to build scientific work flow systems. International workshop on work flow management (IWWM 2009), The institute of electrical and electronics engineers, Inc., May 2009, pp. 27–33
22. CPACS Homepage. http://software.dlr.de/p/cpacs/home/ [cited 31 August 2015]
23. TiXI Homepage. http://software.dlr.de/p/tixi/home/ [cited 31 August 2015]
24. TiGL Homepage. http://software.dlr.de/p/tigl/home/ [cited 31 August 2015]
25. ModelCenter Homepage. http://www.phoenix-int.com/modelcenter/integrate.php [cited 31 August 2015]
26. Seider, D., Fischer, P., Litz, M., Schreiber, A., Gerndt, A.: Open source software framework for applications in aeronautics and space. IEEE Aerospace Conference, March 2012
27. RCE Homepage. http://software.dlr.de/p/rcenvironment/home/ [cited 31 August 2015]
28. Cummings, R., Schütte, A.: An integrated computational/experimental approach to UCAV stability and control estimations: overview of NATO RTO AVT-161. 28th AIAA Applied Aerodynamics Conference, No. AIAA-2010-4392, 2010
29. Becker, R.-G., Wolters, F., Nauroz, M., Otten, T.: Development of a gas turbine performance code and its application to preliminary engine design. DLRK 2011, September 2011
30. VSAERO Homepage. http://www.ami.aero/software-computing/amis-computational-fluid-dynamics-tools/vsaero/ [cited 31 August 2015]
31. Horstmann, K.H.: Ein Mehrfach-Traglinienverfahren und seine Verwendung für Entwurf und Nachrechnung nichtplanarer Flügelanordnungen. Tech. rep., Deutsche Forschungs- und Versuchsanstalt für Luft- und Raumfahrt (1987)
32. Liersch, C.M, Wunderlich, T.F.: A fast aerodynamic tool for preliminary aircraft design. 12th AIAA/ISSMO Multidisciplinary Analysis and Optimization Conference, No. AIAA-2008-5901, September 2008
33. Looye, G.: TECS/THCS-based generic autopilot control laws for aircraft mission simulation. Second CEAS Specialist Conference on Guidance, Navigation and Control, June 2013
34. Krüger, W., Cumnuantip, S., Liersch, C.: Multidisciplinary conceptual design of a UCAV configuration. RTO/AVT Panel Workshop "Virtual Prototyping of Affordable Military Vehicles Using Advanced MDO", 2011
35. Klimmek, T.: Parameterization of topology and geometry for the multidisciplinary optimization of wing structures. CEAS 2009 European Air and Space Conference, October 2009
36. Duus, G., Duda, H.: HAREM—handling qualities research and evaluation using matlab. IEEE International Symposium on Computer Aided Control System Design, Kohala Coast, HI (US), 22–27 August 1999, pp. 428–432
37. Ehlers, J.: Flying qualities analysis of CPACS based aircraft models—HAREM V2.0. Tech. rep., German Aerospace Center (DLR), Institute for Flight Systems, June 2013
38. CATIA Homepage. http://www.3ds.com/de/produkte-und-services/catia/ [cited 31 August 2015]
39. Löser, T., Vicroy, D., Schütte, A.: SACCON static wind tunnel tests at DNW-NWB and 14'x22' NASA LaRC. 28th AIAA Applied Aerodynamics Conference, No. AIAA-2010-4393, 2010
40. Vicroy, D.D., Loeser, T.D., Schütte, A.: Static and forced-oscillation tests of a generic unmanned combat air vehicle. J. Aircr. **49**(6), 1558–1583 (2012)
41. Huber, K.C., Vicroy, D., Schütte, A., Hübner, A.R.: UCAV model design and static experimental investigations to estimate control device effectiveness and Stability and Control capabilities. 32nd AIAA Applied Aerodynamics Conference, No. AIAA-2014-2002, Atlanta, GA, June 2014
42. Galle, M., Gerhold, T., Evans, J.: Technical documentation of the DLR TAU-code. Tech. Rep. DLR-IB 233-97/A43, DLR (1997)
43. Gerhold, T., Friedrich, O., Evans, J., Galle, M.: Calculation of complex three-dimensional configurations employing the DLR-tau-Code. 35th Aerospace Sciences Meeting and Exhibit, January 6–10, 1997, Reno, NV, No. AIAA-1997-0167, January 1997
44. Gerhold, T.: Overview of the hybrid RANS code TAU. In: Kroll, N., Faßbender, J. (eds.) Closing Presentation DLR Project MEGAFLOW, Braunschweig (de), 10.-11.12.2002, Vol. 89 of Notes on Numerical Fluid Mechanics and Multidisciplinary Design (NNFM). Springer, Berlin (2005)
45. Schwamborn, D., Gerhold, T., Heinrich, R.: The DLR TAU-code: recent applications in research and industry. ECCOMAS CFD 2006 Conference, 2006
46. Schütte, A., Huber, K.C., Boelens, O.J.: Static and dynamic numerical simulations of a generic UCAV configuration with and without control devices. 32nd AIAA Applied Aerodynamics Conference, No. AIAA-2014-2132, Atlanta, GA, June 2014
47. Zimper, D., Hummel, D.: Analysis of the transonic flow around a generic UCAV configuration. 32nd AIAA Applied Aerodynamics Conference, No. AIAA-Paper 2014-2266, Atlanta, GA, June 2014
48. Liersch, C.M., Huber, K.C.: Conceptual design and aerodynamic analyses of a generic UCAV configuration. 32nd AIAA Applied Aerodynamics Conference, No. AIAA-Paper 2014-2001, Atlanta, GA, June 2014